PROTEINS
STRUCTURE ■ FUNCTION ■ BIOINFORMATICS

STRUCTURE NOTE

Crystal structure of human carbonic anhydrase-related protein VIII reveals the basis for catalytic silencing

Sarah S. Picaud,[1] João R. C. Muniz,[1] Anneke Kramm,[1] Ewa S. Pilka,[1] Grazyna Kochan,[1] Udo Oppermann,[1,2]* and Wyatt W. Yue[1]*

[1] Structural Genomics Consortium, Old Road Research Campus Building, Oxford, United Kingdom

[2] Botnar Research Centre, Oxford Biomedical Research Unit, Oxford, United Kingdom

Key words: carbonic anhydrase; zinc metalloenzyme; carbon dioxide; bicarbonate.

INTRODUCTION

Carbonic anhydrases (CAs; EC 4.2.1.1) catalyze the reversible hydration of carbon dioxide to bicarbonate and a proton.[1] They are ubiquitous in prokaryotes and eukaryotes, and are encoded by four evolutionarily-unrelated gene classes (α, β, γ, δ). The human CA family belongs to the α class and contains 12 catalytic isozymes with different tissue distribution, subcellular localization and kinetic properties. These include the cytosolic (CA I, CA II, CA III, CA VII, CA XIII), membrane-bound (CA IV, CA IX, CA XII, CA XIV), mitochondrial (CA V_A, CA V_B) and secreted (CA VI) isoforms. They share an absolute requirement for a catalytic Zn^{2+} ion in the active site, coordinated by an hydroxide ion and three invariant histidine residues $H94_{CAII}$, $H96_{CAII}$ and $H119_{CAII}$ (human CA II numbering) that are in turn hydrogen bonded to conserved partners $Q92_{CAII}$, $N244_{CAII}$ and $E117_{CAII}$, respectively. CAs participate in physiological processes such as respiration, metabolite biosynthesis and pH regulation, and are interesting pharmaceutical targets.[2] Sulphonamide-based CA inhibitors are established diuretics and anti-glaucoma drugs, and may have further therapeutic potentials in anti-obesity and anti-cancer treatment.[3]

The human CA family includes a subclass of three noncatalytic isoforms (CA VIII, CA X, CA XI), also known as CA-related proteins (CA-RPs), based on sequence homology with the catalytic isozymes. CA-RPs lack one or more of the essential Zn^{2+}-coordinating histidines and are devoid of CO_2 hydration activity.[4] To date, the biological functions of CA-RPs remain undefined. The first identified CA-RP, CA VIII, replaces the Zn^{2+}-coordinating $H94_{CAII}$ and its hydrogen-bonding partner $Q92_{CAII}$ with R116 and E114, respectively (human CA VIII numbering).[5] CA VIII is highly expressed in the cerebellum,[6] and a mouse gene deletion causes a motor coordination defect.[7] Relevant to this, CA VIII has been identified as a binding partner for the inositol 1,4,5 triphosphate (IP_3) receptor type 1 which is abundant in the cerebellum.[8] To provide insights into the biological properties of CA-RPs, we have determined the 1.6 Å crystal structure of human CA VIII (hCA VIII). This work represents the first structural characterization of a CA-RP and offers a structural basis for its catalytic silencing effect.

Additional Supporting Information may be found in the online version of this article.

*Correspondence to: Udo Oppermann, Structural Genomics Consortium, Old Road Research Campus Building, Oxford, United Kingdom. E-mail: udo.oppermann@sgc.ox.ac.uk or Wyatt Yue, Structural Genomics Consortium, Old Road Research Campus Building, Oxford, United Kingdom. E-mail: wyatt.yue@sgc.ox.ac.uk

Received 29 December 2008; Revised 27 January 2009; Accepted 4 February 2009
Published online 3 March 2009 in Wiley InterScience (www.interscience.wiley.com). DOI: 10.1002/prot.22411

METHODS

Expression, purification and crystallization

A DNA fragment encoding full-length hCA VIII (aa 1–290; GenBank entry 22027500) was subcloned into the pNIC28-Bsa4 vector which incorporates a TEV-cleavable His_6-tag. The plasmid was transformed into BL21(DE3)-pRARE, cultured in 1 L Terrific Broth at 37°C, and induced with 0.1 mM IPTG overnight at 18°C. Cells were homogenized in lysis buffer (50 mM KH_2PO_4 pH 8.0, 500 mM NaCl) and insoluble material was removed by centrifugation. The supernatant was purified by affinity (Ni-sepharose) and size exclusion (Superdex S75) chromatography. Purified protein was treated with His-tagged TEV protease (1:100 v/v) overnight at 4°C, and passed over 1 mL Ni-sepharose resin. Protein was concentrated to 10.5 mg/ml and stored in 10 mM HEPES pH 7.5, 100 mM NaCl, 5% (w/v) glycerol at −80°C.

Crystals were grown at 4°C by vapor diffusion in sitting drops mixing 100 nL protein (10.5 mg/mL) and 200 nL well solution containing 10% (w/v) PEG 6000, 0.3 M NH_4Cl pH 6.3 and 10% (v/v) ethylene glycol. Crystals were cryo-protected using 20% (v/v) ethylene glycol and flash-cooled in liquid nitrogen. Diffraction data to 1.6 Å resolution were collected at the SLS beamline X10SA. Data were indexed and integrated using MOSFLM,[9] and scaled and merged using SCALA from the CCP4 program suite.[10]

Structure determination

Human CA-related protein VIII crystallized in the $P2_12_12_1$ space group with one molecule in the asymmetric unit. The structure was solved by molecular replacement using the program PHASER[11] and the hCA XIII structure (PDB code 3DA2) as search model. Automated model building was performed with ARP/wARP,[12] followed by iterative cycles of restrained refinement and model building using COOT[13] and REFMAC5.[14] The final model consists of aa 24–290, whereas aa 1–23 were not observed in the $2F_o - F_c$ electron density map. During refinement a $F_o - F_c$ difference peak was observed at the bottom of the active site cavity. A chloride ion was modeled into the peak, and refined at full occupancy with B factor comparable with the neighboring protein atoms. Modeling a Zn^{2+} ion into the peak resulted in negative $F_o - F_c$ density. Atomic coordinates and structure factors have been deposited in the PDB under the accession code 2W2J. Data collection and refinement statistics are summarized in Table I. Figures were prepared using PYMOL (www.pymol.org) and ICM Pro (www.molsoft.com).

Table I
Summary of Data Collection and Refinement Statistics

Data collection	
Space group	$P2_12_12_1$
a, *b*, *c* (Å)	44.27, 73.85, 87.91
Wavelength (Å)	1.00
Resolution (Å)[a]	36.99–1.60 (1.69–1.60)
R_{merge} (%)	9.4 (57.8)
$I/\sigma I$	11.5 (1.8)
Completeness (%)	98.1 (87.2)
Redundancy	6.3 (3.7)
Refinement	
Resolution (Å)	34.86–1.60
No. reflections	34701
R_{work}/R_{free} (%)[b]	19.2/22.9
No. atoms	
Protein	2626
Ligand/ion	3
Water	471
B-factors (Å^2)	
Main-chain	22.66
Side-chain and water	30.45
R.m.s deviations	
Bond lengths (Å)	0.007
Bond angles (°)	1.123
Ramachandran plot	
Most favored (%)	96.5
Allowed (%)	3.1
Disallowed (%)	0.4

[a]Numbers in parentheses represent data in the highest resolution shell (1.69–1.60 Å).
[b]R_{free} is calculated for 5.0% of randomly selected reflections excluded from refinement.

RESULTS AND DISCUSSION

Overall structure

The final model of hCA VIII [Fig. 1(A)] comprises part of an N-terminal Glu-rich region (E loop; aa 24–36) that has no counterparts in other CAs, as well as the central core domain (aa 37–290). The first 23 residues were not observed in the electron density map and are presumably disordered. The core domain of hCA VIII adopts the classical architecture of the mammalian CA enzymes, namely a 10-stranded central β-sheet (β11, β4, β5, β7, β9, β10, β13, β12, β15, β2) surrounded by several short α-helices (α1–α3) and β-strands (β1, β3, β6, β8, β14). The overall structure resembles closely the cytosolic isozymes CA II and CA XIII (RMSD 1.3 Å, 41% sequence identity). CA II is a well-characterized isozyme with the highest catalytic turnover.[15] CA XIII has been identified recently[16] and we have determined its structure (PDB code 3DA2; Pilka ES, Picaud SS, Oppermann U, Yue WW, unpublished). Comparison between the hCA VIII and hCA XIII structures reveals significant differences in two loop regions [Fig. 1(B)]. In hCA VIII, the unique E loop protrudes into the exterior and packs against the α3-β15 loop which incorporates a five-residue insertion compared with other isozymes. Together the two loops contribute to an extensive electronegative surface in hCA VIII, which contrasts with the more neutral surface in other isozymes (data not shown).

'Active site' architecture

The catalytic isozymes contain a conical cavity in the core domain with a 15-Å wide entrance, which tapers

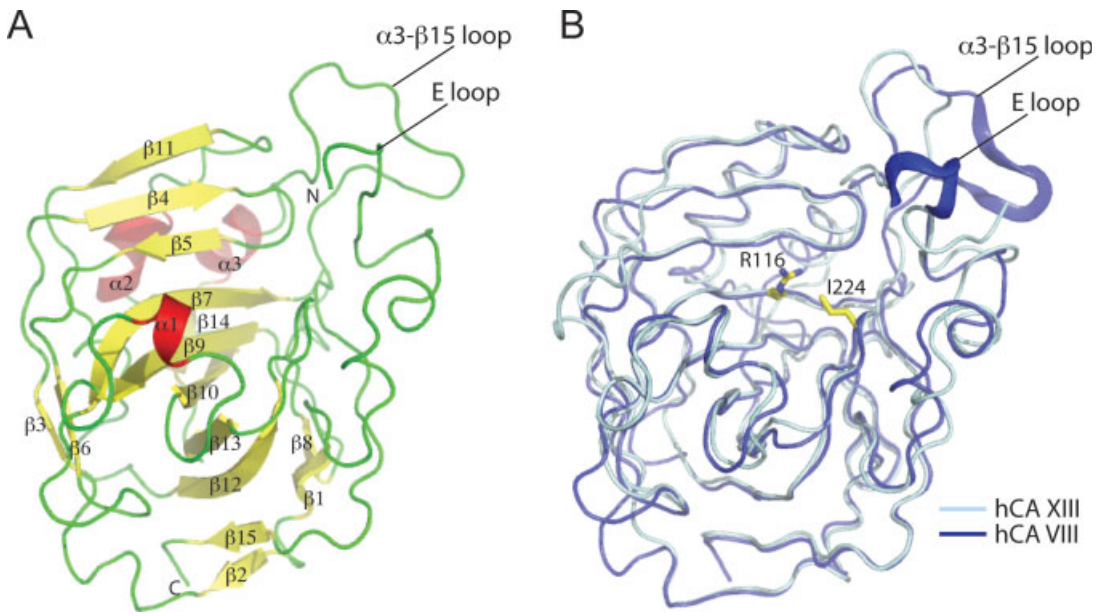

Figure 1

Crystal structure of hCA VIII. (**A**) Ribbon diagram showing the secondary structure elements: α-helices (red) and β-strands (yellow). (**B**) C^{α}-superposition of hCA VIII (blue) and hCA XIII structures (cyan, PDB code 3DA2). The two loop regions that are unique in hCA VIII are shown in thick ribbons.

into the active site at the bottom of the cavity. This cavity provides a crucial transit route for the substrates, products and the Zn^{2+} ion. Compared with other CA structures, the hCA VIII cavity has a much narrower opening because of steric constriction by two bulky residues, R116 and I224, at the cavity entrance [Figs. 1(B) and 2(A)]. R116 replaces the essential Zn^{2+}-coordinating $H94_{CAII}$ and I224 replaces $T200_{CAII}$ conserved in most isozymes [Fig. 2(B)]. Unlike $H94_{CAII}$ side-chain, which points into the active site for Zn^{2+} coordination, the R116 guanidino side-chain of hCA VIII is directed away from the cavity by polar interactions with D85 and E114 [Fig. 2(A)], which correspond to Asn ($N244_{CAII}$) and Gln ($Q92_{CAII}$), respectively, in most isozymes. Remarkably, mutations of R116, E114 and I224 to the corresponding residues in the catalytic isozymes rendered CA VIII enzymatically active.[17,18]

In the catalytic isozymes, the active site constitutes a bipolar binding surface: a hydrophilic face ($T199_{CAII}$, $T200_{CAII}$, $H96_{CAII}$, $H94_{CAII}$, $H119_{CAII}$) which contains the Zn^{2+} binding site and a hydrophobic face ($V121_{CAII}$, $V143_{CAII}$, $L198_{CAII}$, $V207_{CAII}$, $W209_{CAII}$) which harbors the CO_2 substrate pocket [Fig. 2(B), left]. Inspection of the hCA VIII structure reveals significant differences in the equivalent 'active site' [Fig. 2(B), right]. First, the hydrophobic pocket of CA VIII is more spatially constricted due to the substitution of two Val residues ($V121_{CAII}$, $V143_{CAII}$) to Ile (I143, I165). This reduces the pocket size and presumably precludes the binding of CO_2 in the active site. Consistent with this, a $V143_{CAII}$-to-Ile mutation diminished CA II activity by eightfold.[19]

Second, a difference Fourier peak was observed at the bottom of the active site cavity in hCA VIII, close to the position of Zn^{2+} in the catalytic isozymes, but is incompatible with the electronic configuration of Zn^{2+} (see "Materials and methods"). Taking into account (1) the inclusion of NaCl during purification and (2) the absence of Zn^{2+} in the crystallization solution, we have modeled and refined a chloride ion into the density [Fig. 2(B), right]. The Cl^- ion is coordinated by the Nδ1 atom from H118 (bond length 3.02 Å), Nϵ2 atom from H141 (3.01 Å) and a water molecule W15 (3.15 Å). The observed bond lengths are significantly different from the typical Zn^{2+} coordination [Fig. 2(C)], but are consistent with the observed noncovalent Cl–N bond distances (2.9–3.2 Å) from our survey of PDB structures (resolution <2.0 Å, modeled with Cl^-; data not shown). Selected examples from the PDB with observed Cl^--histidine interactions are listed in Table S1 of the Supporting Information.

Biological perspective

Our structural data revealed that CA VIII evolves to adopt the classic CA fold but substitutes key residues in the active site cavity that preclude the entry and binding of the catalytic Zn^{2+} and substrate CO_2, hence silencing its activity. Nevertheless, the high sequence conservation

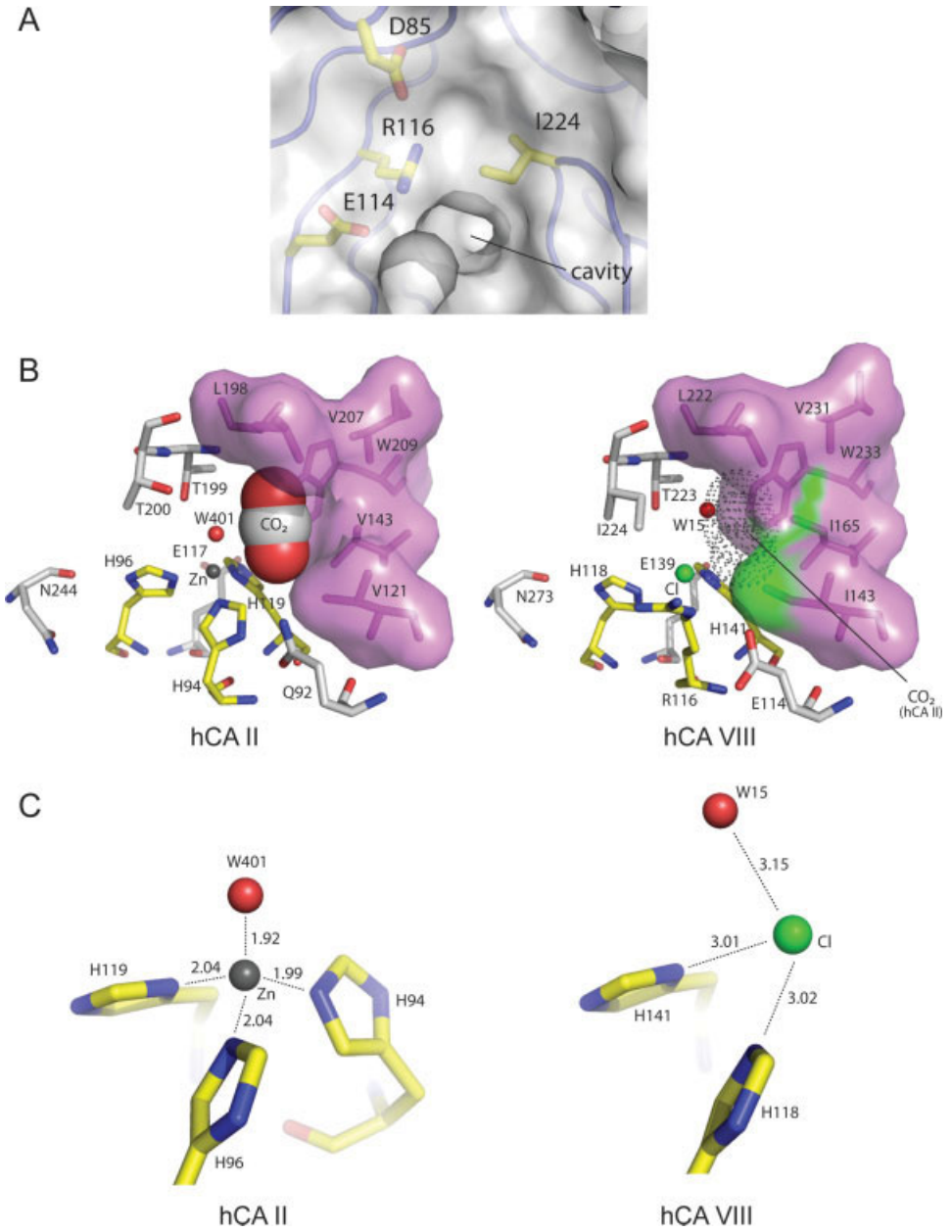

Figure 2

Structural comparison of hCA VIII with the catalytic isozymes. (**A**) A close-up view showing the entrance of the hCA VIII cavity. hCA VIII is represented in blue ribbon, overlayed with a surface representation. (**B**) Active site of the CO_2-bound hCA II (left, PDB code 3D92) and hCA VIII (right) structures. The hydrophobic CO_2 pocket is shown in pink surface. Spheres represent the Zn^{2+} ion (black), water (red) and Cl^- ion (green). In the right panel, the CO_2 substrate from the hCA II structure (shown in dots) is superimposed onto the hCA VIII structure to illustrate the potential steric clash caused by I165 and I143 (green surface). (**C**) Schematic representation of the Zn^{2+} coordination in hCA II (left), and Cl^- coordination in hCA VIII (right). Bond lengths are indicated in Å.

between human and mouse CA VIII homologs (98% identity) lends support to the hypothesis that over the course of evolution the absence of CA activity may be associated with the gain of a new, yet unidentified cellular function for CA VIII. One possibility is the modulation of biological functions via protein–protein interactions. The type 1 IP_3 receptor, identified as a CA VIII-binding protein, contains an electropositive IP_3 binding site.[20] It is possible that the electronegative surface in CA VIII, unique among CAs, may form a charge-complementary binding site for the receptor, thereby regulating IP_3-dependent Ca^{2+} release.[7] Consistent with this, a pro-

tein-interaction function has been reported for the CA-like domain in receptor protein tyrosine phosphatase β which serves as the contactin binding site.[21]

ACKNOWLEDGMENTS

The Structural Genomics Consortium is a registered charity (Number 1097737) funded by the Canadian Institutes for Health Research, the Canadian Foundation for Innovation, Genome Canada through the Ontario Genomics Institute, GlaxoSmithKline, Karolinska Institutet, the Knut and Alice Wallenberg Foundation, the Ontario Innovation Trust, the Ontario Ministry for Research and Innovation, Merck and Co., Inc., the Novartis Research Foundation, the Swedish Agency for Innovation Systems, the Swedish Foundation for Strategic Research and the Wellcome Trust.

REFERENCES

1. Lindskog S. Structure and mechanism of carbonic anhydrase. Pharmacol Ther 1997;74:1–20.
2. Supuran CT. Carbonic anhydrases: novel therapeutic applications for inhibitors and activators. Nat Rev Drug Discov 2008;7:168–181.
3. Supuran CT. Carbonic anhydrases as drug targets—an overview. Curr Top Med Chem 2007;7:825–833.
4. Tashian RE, Hewett-Emmett D, Carter ND, Bergenhem NCH. Carbonic anhydrase (CA) related proteins (CA-RPs), and transmembrane proteins with CA or CA-RP domains. In: Chegwidden WR Carter ND, Edwards YH, editors. The carbonic anhydrases new horizons. Basel: Birkhauser; 2000. pp 105–120.
5. Bergenhem NC, Hallberg M, Wisen S. Molecular characterization of the human carbonic anhydrase-related protein (HCA-RP VIII). Biochim Biophys Acta 1998;1384:294–298.
6. Lakkis MM, Bergenhem NC, O'Shea KS, Tashian RE. Expression of the acatalytic carbonic anhydrase VIII gene. Car8, during mouse embryonic development. Histochem J 1997;29:135–141.
7. Jiao Y, Yan J, Zhao Y, Donahue LR, Beamer WG, Li X, Roe BA, Ledoux MS, Gu W. Carbonic anhydrase-related protein VIII deficiency is associated with a distinctive lifelong gait disorder in waddles mice. Genetics 2005;171:1239–1246.
8. Hirota J, Ando H, Hamada K, Mikoshiba K. Carbonic anhydrase-related protein is a novel binding protein for inositol 1,4,5-trisphosphate receptor type 1. Biochem J 2003;372(Pt 2):435–441.
9. Leslie AGW. Recent changes to the MOSFLM package for processing film and image plate data. Joint CCP4 + ESF-EAMCB Newsletter on Protein Crystallography 1992;26.
10. CCP4. The CCP4 suite: programs for protein crystallography. Acta Crystallogr D Biol Crystallogr 1994;50(Pt 5):760–763.
11. McCoy AJ, Grosse-Kunstleve RW, Storoni LC, Read RJ. Likelihood-enhanced fast translation functions. Acta Crystallogr D Biol Crystallogr 2005;61(Pt 4):458–464.
12. Perrakis A, Harkiolaki M, Wilson KS, Lamzin VS. ARP/wARP and molecular replacement. Acta Crystallogr D Biol Crystallogr 2001; 57(Pt 10):1445–1450.
13. Emsley P, Cowtan K. Coot: model-building tools for molecular graphics. Acta Crystallogr D Biol Crystallogr 2004;60(Pt 12):2126–2132.
14. Murshudov GN, Vagin AA, Dodson EJ. Refinement of macromolecular structures by the maximum-likelihood method. Acta Crystallogr D Biol Crystallogr 1997;53(Pt 3):240–255.
15. Briganti F, Mangani S, Orioli P, Scozzafava A, Vernaglione G, Supuran CT. Carbonic anhydrase activators: X-ray crystallographic and spectroscopic investigations for the interaction of isozymes I and II with histamine. Biochemistry 1997;36:10384–10392.
16. Lehtonen J, Shen B, Vihinen M, Casini A, Scozzafava A, Supuran CT, Parkkila AK, Saarnio J, Kivela AJ, Waheed A, Sly WS, Parkkila S. Characterization of CA XIII, a novel member of the carbonic anhydrase isozyme family. J Biol Chem 2004;279:2719–2727.
17. Sjoblom B, Elleby B, Wallgren K, Jonsson BH, Lindskog S. Two point mutations convert a catalytically inactive carbonic anhydrase-related protein (CARP) to an active enzyme. FEBS Lett 1996;398: 322–325.
18. Elleby B, Sjoblom B, Tu C, Silverman DN, Lindskog S. Enhancement of catalytic efficiency by the combination of site-specific mutations in a carbonic anhydrase-related protein. Eur J Biochem 2000;267:5908–5915.
19. Fierke CA, Calderone TL, Krebs JF. Functional consequences of engineering the hydrophobic pocket of carbonic anhydrase II. Biochemistry 1991;30:11054–11063.
20. Bosanac I, Alattia JR, Mal TK, Chan J, Talarico S, Tong FK, Tong KI, Yoshikawa F, Furuichi T, Iwai M, Michikawa T, Mikoshiba K, Ikura M. Structure of the inositol 1,4,5-trisphosphate receptor binding core in complex with its ligand. Nature 2002;420:696–700.
21. Peles E, Schlessinger J, Grumet M. Multi-ligand interactions with receptor-like protein tyrosine phosphatase beta: implications for intercellular signaling. Trends Biochem Sci 1998;23:121–124.